Cement & Concrete Composites 32 (2010) 468–477

Contents lists available at ScienceDirect

Cement & Concrete Composites

journal homepage: www.elsevier.com/locate/cemconcomp

A multi-phase kinetic model to simulate hydration of slag–cement blends

Xiao-Yong Wang [a], Han-Seung Lee [a,*], Ki-Bong Park [b], Jae-Jun Kim [c], Jay S. Golden [d]

[a] *School of Architecture & Architectural Engineering, Hanyang University, Ansan 425-791, Republic of Korea*
[b] *Division of Architecture, College of Engineering, Kangwon National University, Chuncheon 200-701, Republic of Korea*
[c] *School of Architecture & Architectural Engineering, Hanyang University, Seoul, Republic of Korea*
[d] *School of Sustainability, Civil and Environmental Engineering, Arizona State University, United States*

ARTICLE INFO

Article history:
Received 7 October 2008
Received in revised form 17 March 2010
Accepted 17 March 2010
Available online 21 March 2010

Keywords:
Slag reaction
Cement hydration
Blended cement
Simulation

ABSTRACT

Ground granulated blast furnace slag, which shows cementitious behavior (latent hydraulic activity) and pozzolanic characteristics (reaction with lime), has been widely used as a mineral admixture in normal and high strength concretes. Hydration of slag–blended cement is much more complex than that of ordinary Portland cement because of the mutual interactions between the cement hydration and the slag reaction. This paper presents a kinetic hydration model for cement–slag blends. The proposed model analyzes the slag reaction separate from cement hydration by considering the production of calcium hydroxide in cement hydration and its consumption in slag reactions. The amount of free water and the amount of calcium hydroxide left in the system were adopted as the control indicators for determining the slag reaction. Using the proposed model, the reaction ratio of slag can be evaluated as a function of curing age, considering the influences of the water to binder ratio, the slag replacement ratio and the curing temperature. Furthermore, the amount of chemically-bound water (self-cementing properties), calcium hydroxide (pozzolanic capabilities), and the heat released from hydration are evaluated by determining the contributions from both the cement hydration and the slag reaction. The evaluated results show good accordance with the experimental results.

1. Introduction

Ground granulated blast furnace slag (GGBFS) is a glassy, granular material consisting of silicates, aluminosilicate of calcium and other oxides. Ground granulated blast furnace slag shows both cementitious behavior (latent hydraulic activity) and some pozzolanic characteristics (reaction with lime) as well. It has long been used as a mineral admixture to produce and improve the durability of high strength, high performance concrete. In addition, economic and ecologic benefits in the form of energy-saving and resource-conserving properties can be achieved by using slag–blended cement [1,2].

Experimental and practical studies on the influence of slag on concrete's durability and mechanical properties are abundant. Shi and Day [3] and Song et al. [4] reported that the initial pH value of the activator solution plays an important role in dissolving the slag and in promoting the early formation of some hydration products. Wang and Scrivener [5] reported that regardless of the activator used, the main hydration products of alkali–activated slag are calcium silicate hydrates with low C/S ratios, and Chen and Brouwers [6] proposed a reaction model for alkali–activated slag. Stoichiometric reaction models have been developed in order to correlate the mineral composition of slag with the hydration products. Using the proposed models, it is possible to determine the quantities of the hydration products and the composition of the calcium silicate hydrate (C–S–H).

Compared with alkali–activated slag, the slag–blended cement hydration process is more complex, due to the coexistence of cement hydration and slag reaction. Based on the experimental results of reaction stoichiometries among supplementary cementing materials (SCM), chemical bound water and calcium hydroxide, Papadakis [7], Papadakis and Tsimas [8], and Papadakis et al. [9,10] proposed a chemical-based steady-state model which was able to estimate the final material values, such as porosity, chemically-bound water and calcium hydroxide content, while hydrating the supplementary cementing materials (SCM) of blended cement. The influence of mineral admixture on the durability properties, such as chloride attack and carbonation, and on the strength characteristics were also described quantitatively. However, on the construction site, workers and designers are interested in not only the final properties of slag–blended concrete, but also the evolution of the properties over time. Contrasting to Papadakis' chemical-based steady-state model [7–10], some kinetic models [11–20] were proposed to evaluate the development of properties of blended concrete. Schindler and Folliard [11] proposed a general kinetic hydration model that could predict the heat evolution of cementitious materials. This proposed model incorporated the

---

* Corresponding author. Tel./fax: +82 31 400 5181.
E-mail address: ercleehs@hanyang.ac.kr (H.-S. Lee).

0958-9465/$ - see front matter © 2010 Elsevier Ltd. All rights reserved.
doi:10.1016/j.cemconcomp.2010.03.006

effects of cement mineral composition, cement fineness, supplementary cementing materials, mixture proportions, and concrete properties. De Schutter and Taerwe [12,13] and De Schutter [14–16] proposed a kinetic hydration model valid both for Portland cement and blast furnace slag cement in which the heat evolution of blast furnace slag cement was obtained through the superposition of the heat productions for the Portland reaction (P reaction) and a slag reaction (S reaction). Furthermore, Schutter evaluated the evolution of the mechanical properties of young concrete with respect to the degrees of hydration and the risk of thermal cracking in the hardening concrete. However, it should be noticed that Schutter's model does not explicitly consider the interactions between the cement hydration and the reaction of mineral admixtures, such as the producing of calcium hydroxide by cement hydration and the consumption by slag reaction. Hyun [17] and Tomosawa et al. [18] proposed a kinetic model of slag–blended cement hydration in order to evaluate the early-age temperature rise and the evolution of thermal stress inside a mass of concrete. In this model, the residual concentration of water and calcium hydroxide was used as parameters for indicating the rate decline toward the reaction end point. The influence of temperature on cement hydration is analyzed using Arrhenius's law [18]. Maekawa et al. [19] proposed a general hydration model (DuCOM) incorporating fly ash and slag, whose reactions were treated separately from those of ordinary Portland cement, with some of the interactions being taken into account in terms of the free water content and the calcium hydroxide concentration. Most recently, Di Luzio and Cusatis [20,21] proposed a hydrothermal chemical model for high performance concrete. The Pozzolanic reaction of silica fumes was modeled using a kinetic equation similar to that used for cement hydration.

Based on the review of current literature [7–21], it is obvious that the reaction ratio of mineral admixtures plays a critical role in evaluating both the early-age properties [11–20], such as temperature increase and thermal cracks, and the durability of blended concrete [19,20], as measured by porosity and the amount of calcium hydroxide, both of which are related to the carbonation of concrete. The reaction ratio of slag is related to its physical and chemical characteristics, its mixing proportions, and its curing conditions. In this study, based on a similar idea proposed by Maekawa et al. [19], a kinetic hydration model was used to evaluate the reaction ratio of slag, considering the mutual interactions between cement hydration and slag reaction. The amount of free water and calcium hydroxide left in the system were adopted as the control indicators for the slag reaction. By applying the proposed model, the reaction ratio of slag was evaluated as a function of the curing age, taking into account the influence of the water to binder ratio, the slag replacement ratio and the curing temperature. Furthermore, the amount of chemically-bound water (self-cementing properties), calcium hydroxide (pozzolanic capabilities), and the released heat of hydration were determined by evaluating the contributions from both the cement hydration and the slag reaction.

2. Hydration model of ordinary Portland cement

2.1. Hydration model assumptions

In our hydration model we considered the hydration reaction of Portland cement in terms of the influence of the water to cement ratio, the cement particle size distribution, the cement mineral components and the curing temperature. The assumptions of this model are summarized as follows:

1. Cement particles are randomly cast in a representative unit cell space, as shown in Fig. 1. As proposed by Navi and Pignat [22], the length of the edge of the representative unit cell is 100 μm. Our simulation assumed the amount of chemically-bound water for each cement component, C_3S, C_2S, C_3A, and C_4AF, was the same as those proposed by Park et al. [23].

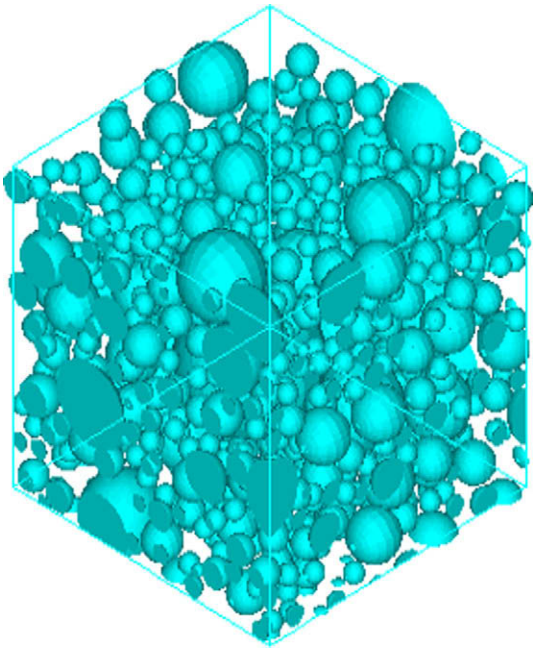

Fig. 1. Cement particles randomly distributed in the cell space.

2. The degree of hydration of the cement components is the ratio of the volume of reacted cement components to the volume of initial cement components. The degree of hydration of cement paste can be regarded as a weighted sum of the cement particles and the mineral components, as shown in Fig. 2.
3. The liquid phase, which was assumed to be water, diffuses through a hydrate layer, reaches the surface of the cement particle and chemically reacts with the cement. The hydrate formed by hydration adheres spherically to the cement particles.
4. The particle size distribution of the cement was approximated using the Rosin–Rammler function [23].

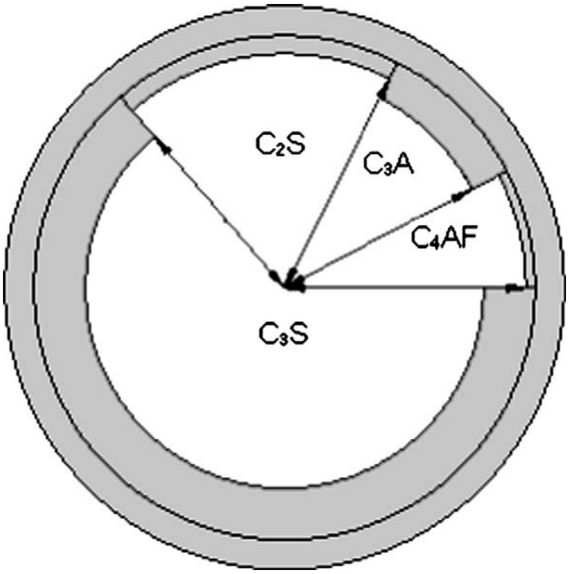

Fig. 2. Schematic of the multi-component hydration model.

2.2. Hydration mechanisms

Park's model [23] showed an improved performance by incorporating the size distribution of cement particles and the components of the cement minerals, including C_3S, C_2S, C_3A and C_4AF. The basic hydration equation for each mineral composition in the cement particles can be described by Eq. (1), which was originally used by Tomosawa [24] to describe the hydration of a single cement particle. This model is expressed as a single equation composed of four rate determining coefficients which consider the rate of formation and the destruction of the initial impermeable layer, the activated chemical reaction process and the subsequent diffusion-controlled process:

$$\frac{d\alpha_i^j}{dt} = \frac{3C_{w\infty}}{(v_i + w_{ag})r_0^j\rho_i}\frac{1}{\left(\frac{1}{k_d} - \frac{r_0^j}{D_{ei}}\right) + \frac{r_0^j}{D_{ei}}\left(1 - \alpha_i^j\right)^{\frac{-1}{3}} + \frac{1}{k_{ri}}\left(1 - \alpha_i^j\right)^{\frac{-2}{3}}}, \tag{1}$$

where α_i^j denotes the degree of hydration for the mineral components in a given cement particle, i is the mineral component, j is the number of cement particles, v_i is the stoichiometric ratio showing the mass of water to the mass of mineral components, w_{ag} is the physically-bound water that is equal to approximately 15% of the mass of the reacted cement, ρ_i is the density of the anhydrate cement mineral component, k_d is the reaction coefficient in the dormant period, r_0^j is the radius of the anhydrate cement particles, D_{ei} is the effective diffusion coefficient of water in the hydration product for each mineral component, k_{ri} is the coefficient of the reaction rate for each mineral component, and $C_{w\infty}$ is the abundance concentration of water at the outer region of the gel. Furthermore, k_d is assumed to be a function of the degree of hydration during the initial reaction period and is expressed by:

$$k_d = \frac{B}{\left(\alpha_i^j\right)^{1.5}} + C\left(r_0^j - r_t^j\right)^4, \tag{2}$$

where B and C are the reaction coefficients.

The effective diffusion coefficient of water is affected by the tortuosity and the radius of the hydrate gel pore. This phenomenon can be expressed as a function of the degree of hydration and is described by:

$$D_{ei} = De_{i0}\ln\left(\frac{1}{\alpha_i^j}\right). \tag{3}$$

The influence of temperature on cement hydration can be analyzed using Arrhenius's law [18] as follows:

$$B = B_{20}\exp\left(-\beta_1\left(\frac{1}{T} - \frac{1}{293}\right)\right), \tag{4}$$

$$D_{ei} = D_{ei20}\exp\left(-\beta_{2i}\left(\frac{1}{T} - \frac{1}{293}\right)\right), \tag{5}$$

$$k_{ri} = k_{ri20}\exp\left(-\frac{E_i}{R}\left(\frac{1}{T} - \frac{1}{293}\right)\right), \tag{6}$$

where B_{20}, D_{ei20}, and k_{ri20} are the values of B, D_{ei} and k_{ri} at 293 K, respectively, and β_1, β_{2i} and E_i/R are the activation energies of B, D_{ei} and k_{ri}, respectively. The activation energies of each compound were obtained from cement hydration experiments performed under different curing temperatures.

When the cement was mixed with water, the hydration of each of the mineral components occurs according to the model described in the previous section. The degree of cement hydration can be calculated as follows:

$$\alpha = \frac{\sum_{j=1}^{j=n}\sum_{i=1}^{i=4}\alpha_i^j g_i g_j}{\sum_{j=1}^{j=n}\sum_{i=1}^{i=4} g_i g_j}, \tag{7}$$

where g_i is the mass fraction of each mineral component, g_j is the mass fraction of the individual particles in the cement, and n is the total number of cement particles in a cell space. As shown in Eq. (7), the different hydration reactions do not consume the same amount of water; therefore, the computation of the total consumed water should be a weighted average of the consumed water for each elementary reaction.

2.3. Water withdrawal mechanism

During the hydration period, at a certain point in time after the initial setting time, due to the increasing interconnections among the cement particles, the contact area between a cement particle and the surrounding water will decrease, resulting in a slower hydration rate. Powers [25] proposed that the water present in the paste can be classified into evaporable and non-evaporable fractions. The former represents the capillary and gel waters that partially reside within the hydration product. The non-evaporable water is defined as the bound water that has chemically reacted with the cement. During the hydration process, only the capillary water contributes to further hydration, during which it will be consumed, and the relative hydration rate will decrease. Under sealed-curing conditions, when the water to cement ratio is less than 0.38, due to the limited supply of capillary water, cement hydration cannot be completed [25]. In this condition, the chemically-bound water mass is approximately equal to 23% of the reacted cement mass, and the gel water mass is equal to approximately 15% of the reacted cement mass.

Considering these two aforementioned factors, proposed by Park et al. [23] and Maruyama [26], we modified Eq. (1) as follows:

$$\left(\frac{d\alpha_i^j}{dt}\right)' = \frac{d\alpha_i^j}{dt}\left(\frac{\text{free surface}}{\text{total surface}}\right)^j\frac{\text{capillary water}}{w_0}, \tag{8.1}$$

$$\text{Capillary water} = w_0 - 0.38Ce_0\alpha, \tag{8.2}$$

where w_0 is the water mass, Ce_0 is the cement mass in the mixing proportions, and $\frac{w_0 - 0.38 * Ce_0 * \alpha}{w_0}$ considers the decrease in the available capillary water for cement hydration. The term $\left(\frac{\text{free surface}}{\text{total surface}}\right)^j$ represents the ratio between the free surface area (the area in contact with the water) and the total surface area, which can be determined using the method proposed in [22].

3. Hydration model for slag–blended cement

3.1. Calcium hydroxide (CH) and capillary water amounts during the hydration process

As proposed by Papadakis [7], Papadakis and Tsimas [8], and Papadakis et al. [9,10], during the hydration period the chemical reactions of the mineral components in Portland cement can be expressed as follows:

$$2C_3S + 6H \rightarrow C_3S_2H_3 + 3CH, \tag{9.1}$$

$$2C_2S + 4H \rightarrow C_3S_2H_3 + CH, \tag{9.2}$$

$$C_3A + C\bar{S}H_2 + 10H \rightarrow C_4A\bar{S}H_{12}, \tag{9.3}$$

$$C_4AF + 2CH + 10H \rightarrow C_6AFH_{12}. \tag{9.4}$$

It is possible to determine the mass per unit volume for each hydration product of Portland cement, such as calcium hydroxide and C–S–H, using the aforementioned hydration model and Eqs. (9.1)–(9.4), in conjunction with:

$$CH = 74.1Ce_0(1.5g_{c3s}\alpha_{c3s} + 0.5g_{c2s}\alpha_{c2s} - 2g_{c4af}\alpha_{c4af}), \tag{10.1}$$

$$CSH = 342.1Ce_0(1.5g_{c3s}\alpha_{c3s} + 0.5g_{c2s}\alpha_{c2s}). \tag{10.2}$$

Ground granulated blast furnace slag often contains more than 95% glass, while some minor crystalline phases may exist. Only the glass part of the slag has latent hydraulic properties, as the crystalline phases remain intact during hydration [5]. The main crystalline phases in slag are merwinite (C_3MS_2) and melilite, the latter of which is a solid solution of gehlenite (C_2AS) and akermanite phases (C_2MS_2). Many XRD studies have shown that the principal hydration products of slag are similar to those of pure Portland cement [2], but the quantities of CH found by this or other methods are in varying degrees lower than those which would be given by the Portland cement if the slag took no part in the reaction. When a higher percentage of slag is used, the CH content may pass through a maximum level and then decrease [2]. In addition, the retained water in the slag hydration products is higher than that in Portland cement. To achieve a high degree of slag hydration, a larger initial water/binder ratio is optimal [7].

Maekawa et al. [19] conducted a systematic investigation of the hydration, microstructure formation and mass transport of both Portland concrete and blended concrete. Based on this analysis of the experimental results of the chemically-bound water amounts, the adiabatic temperature rise tests, and the temperature measurements of small quasi-adiabatic blocks, Maekawa et al. [19] proposed that the reaction of slag can be roughly described by the following approximate key values:

Chemically-bound water	0.30 g/g reacted slag
Gel water	0.15 g/g reacted slag
Calcium hydroxide	0.22 g/g reacted slag

Based on the hydration model and the stoichiometry of the slag reaction proposed by Maekawa et al. [19], the amounts of calcium hydroxide, chemically-bound water and capillary water present during the hydration period can be determined as follows:

$$\mathrm{CH} = 74.1Ce_0(1.5g_{c3s}\alpha_{c3s} + 0.5g_{c2s}\alpha_{c2s} - 2g_{c4af}\alpha_{c4af}) - 0.22\gamma\alpha_{\mathrm{glass}}P, \tag{11.1}$$

$$\text{Capillary water} = w_0 - 0.38Ce_0\alpha - 0.3\gamma\alpha_{\mathrm{glass}}P - 0.15\gamma\alpha_{\mathrm{glass}}P, \tag{11.2}$$

$$\text{Chemically-bound water} = 0.23Ce_0\alpha + 0.3\gamma\alpha_{\mathrm{glass}}P. \tag{11.3}$$

In Eqs. (11.1)–(11.3), γ represents the glass portion of slag, α_{glass} is the reacted degree of the active (glass) portion of the slag, $\gamma\alpha_{\mathrm{glass}}$ is the reacted ratio of slag including both the glass and crystalline phases, and P is the slag mass in the mixing proportion. As shown in Eq. (11.1), the evolution of the calcium hydroxide mass is dependent on two factors, the production of calcium hydroxide from the hydration of the Portland cement and its consumption during the slag reaction. Eq. (11.2) shows the amount of capillary water consumed by both cement hydration and slag reaction. Eq. (11.3) indicates that both Portland cement hydration and the slag reaction contribute to the amount of chemically-bound water.

3.2. The simulation of the slag reaction in cement–slag blends

The addition of slag has both physical and chemical effects on cement hydration. The physical aspects include delay and nucleation effects, and the chemical aspect results in reaction activity, such as self-cementing properties and pozzolanic capabilities. As introduced by Gutteridge and Dalziei [27], slag may affect the chemical composition of the pore solution and may delay the length of the dormant period. However, this delay can be partly compensated for by the nucleation effect. The slag particles can serve as nucleic sites for the cement particles, leading to the chemical activation of cement hydration. In fact, as proposed by Paine et al. [28], in the hydration process of cement–slag blends, the influences of delay and acceleration effects on heat evolution are not significant and, for practical purposes, can be ignored. Therefore, the physical effects were not considered in this paper, but will be addressed in future research. In contrast to the physical effects, the reaction activity of slag has a dominant effect on the properties of slag–concrete. This paper focuses on the simulation of the reaction activity in slag–blended cement hydration. In addition to the physical and chemical effects, when cement is partially replaced by the same quantity of slag, the amount of cement will decrease and the water to cement ratio will increase. This effect can be considered using the cement hydration model, shown as Eq. (8).

The proposed model is founded on the mechanistic similarities in the cement hydration and slag reactions. The first of these is that the cements reacting with water and the glass phase of the slag both possess self-cementing properties and pozzolanic capabilities. The cement hydration process includes an initial dormant period, a phase-boundary reaction period and a diffusion period. In the late stages of cement hydration, diffusion becomes the controlling process. Some researchers have argued that the reaction of mineral admixtures is a diffusion-controlled process [29]. The second mechanistic similarity is based on analyses of SEM micrographs of Portland cement paste, slag–cement paste and fly ash–cement paste, as researchers [7–10,30] have reported that the cement hydration product adheres to the surface of the cement particles, and that the reaction products of the fly ash or slag adhered to the surfaces of the remaining fly ash or slag particles. Furthermore, small-sized cement particles have a high reactivity to water and show almost no initial dormant period, whereas large-sized cement particles did show initial dormant periods [23]. Similarly, silica fume, a highly pozzolanic cement replacement material, showed only a short initial dormant period, similar to that of a small cement particle. Slag also showed an initial dormant period [12–16], due to the fact that slag activation occurs predominantly in the breaking down of its glass phase. The pH value required to dissolve slag is approximately 11.5 or higher [4]. However, there also exist some differences between the cement hydration and slag reactions. Cement hydration will produce calcium hydroxide, whereas the slag reaction will consume it. As proposed by Saeki and Monteiro [31], the hydration rate of the mineral admixtures depends on the amount of calcium hydroxide in the hydrating blends and the relative reaction stage of the mineral admixture. Thus, it is possible to derive an equation describing the process from cement hydration to slag reaction by considering both the similarities and differences between the two reactions.

In our simulation, we assumed that the slag reaction was divided into three processes: an initial dormant period, a phase-boundary reaction process and a diffusion process. Based on the method proposed by Saeki and Monteiro [31], the reaction equation of the active (glass) portion in slag can be written as:

$$\frac{d\alpha_{\mathrm{glass}}}{dt} = \frac{m_{CH}(t)}{P}\,\frac{\text{capillary water}}{w_0}\,\frac{3}{\upsilon_{SL}r_{SL0}\rho_{SL}}\,\frac{1}{\left(\frac{1}{k_{dSL}} - \frac{r_{SL0}}{D_{eSL}}\right) + \frac{r_{SL0}}{D_{eSL}}(1-\alpha_{\mathrm{glass}})^{\frac{-1}{3}} + \frac{1}{k_{rSL}}(1-\alpha_{\mathrm{glass}})^{\frac{-2}{3}}}, \tag{12.1}$$

$$k_{dSL} = \frac{B_{SL}}{(\alpha_{\mathrm{glass}})^{1.5}} + C_{SL}(\alpha_{\mathrm{glass}})^3, \tag{12.2}$$

$$D_{eSL} = D_{eSL0}\ln\left(\frac{1}{\alpha_{\mathrm{glass}}}\right), \tag{12.3}$$

where $m_{CH}(t)$ represents the calcium hydroxide mass in a unit volume of hydrating cement–slag blend and can be obtained from Eq. (11.1), P is the slag mass in the mixing proportion, capillary water is the mass of capillary water and can be obtained from Eq. (11.2), υ_{SL} is the stoichiometry ratio of the mass of CH to the mass of slag, r_{SL0}

is the radius of the slag particle, ρ_{SL} is the slag density, k_{dSL} is the reaction rate coefficient in the dormant period with the coefficients of B_{SL} and C_{SL}, D_{eSL0} is the initial diffusion coefficient, and k_{rSL} is the reaction rate coefficient. The influence of temperature on hydration was considered using Arrhenius's law as follows:

$$B_{SL} = B_{SL20} \exp\left(-\beta_{1SL}\left(\frac{1}{T} - \frac{1}{293}\right)\right), \tag{13}$$

$$C_{SL} = C_{SL20} \exp\left(-\beta_{2SL}\left(\frac{1}{T} - \frac{1}{293}\right)\right), \tag{14}$$

$$D_{eSL0} = D_{eSL20} \exp\left(-\beta_{3SL}\left(\frac{1}{T} - \frac{1}{293}\right)\right), \tag{15}$$

$$k_{rSL} = k_{rSL20} \exp\left(-\frac{E_{SL}}{R}\left(\frac{1}{T} - \frac{1}{293}\right)\right), \tag{16}$$

where B_{SL20}, C_{SL20}, D_{eSL20}, and k_{rSL20} are the values of B_{SL}, C_{SL}, D_{eSL} and k_{rSL} at 293 K, respectively, and β_{1SL}, β_{2SL}, β_{3SL} and E_{SL}/R are the activation energies of B_{SL}, C_{SL}, D_{eSL} and k_{rSL}, respectively. The activation energy of the slag reactions in cement–slag blends can be determined using hydration experiments performed on cement–slag blends for different curing temperatures.

The released heat of the hydrating blends is due to the released heat from the Portland cement hydration and the released heat from the slag reactions. The total released heat is expressed as:

$$\frac{dQ}{dt} = Ce_0 \, * \sum g_i H_i \frac{d\alpha_i}{dt} + P \, * \, H_{SL} * \frac{d\alpha_{\text{glass}} \, * \, \gamma}{dt}, \tag{17}$$

where the first term represents the Portland cement hydration and the second term is the slag reaction, and H_i and H_{SL} are the specific heat generation contents of the individual components [19]. The value of H_{SL} was proposed as 110 kcal/kg, and the specific heat generation content of slag was set by comparing the analytical results with the experimental data [19].

The porosity of the hydrating blends was reduced due to the Portland cement hydration and the slag reaction during the hydration period. As proposed by Papadakis [7], Papadakis and Tsimas [8], and Papadakis et al. [9,10], porosity can be determined as:

$$\varepsilon = \frac{w_0}{\rho_w} - \Delta\varepsilon_h - \Delta\varepsilon_p, \tag{18}$$

where $\Delta\varepsilon_h$ is the porosity reduction due to the hydration of Portland cement, which can be obtained from the amount of chemically-bound water consumed during the hydration of the Portland cement, $\Delta\varepsilon_p$ is the porosity reduction due to the slag reaction and can be obtained from the amount of chemically-bound water consumed in the slag reaction.

4. Results and discussion

4.1. The degree of mineral component hydration in ordinary Portland cement

In this section, we describe the process in which the experimental results for the degree of hydration for ordinary Portland cement were used to calibrate the coefficients of our hydration model [32]. The water to cement ratio was 0.5 and the curing temperatures were 283 K, 293 K and 313 K. The hydration degree of the mineral components was measured at 1, 3, 7, 28, 91, 190 and 365 days. Powder X-ray diffraction/Rietveld analysis was used to measure the degrees of hydration of the cement mineral components. By a regression of the experimental results, the reaction coefficients of the multi-component hydration model were obtained and are listed in Table 1.

Fig. 3 shows a comparison between the experiment results and the calculated results. Because the reaction rates of C_3S and C_3A were much quicker than those of C_2S and C_4AF, the hydrations of C_3S and C_3A reached a steady state much earlier than did those of C_2S and C_4AF. Most of the C_3A and C_3S reacted in the first 1000 h. As shown in Fig. 3, the calculated results agreed overall with the experimental results. Using the degrees of hydration of the individual mineral components, the global degree of hydration was obtained using Eq. (7). Using Eqs. (10.1) and (10.2), the masses of calcium hydroxide and C–S–H in a unit volume during the hydration period were able to be obtained. In Figs. 4 and 5, the masses of calcium hydroxide and C–S–H are shown as a function of the degree of hydration. It is obvious that the CH and C–S–H masses were almost linearly dependent on the hydration degree. By measuring the amounts of calcium hydroxide and combined water, Saeki and Monteiro [31] also found that the CH content linearly depended on the degree of hydration.

4.2. The hydration of slag–blended cement

In this section, we describe the experimental results of the hydration of cement–slag blends [33], are adopted to calibrate and validate the proposed hydration model. The chemical compositions of Portland cement and slag are shown in Tables 2 and 3, respectively. Pastes of slag–blended cements with 30% and 50% slag and water to solids ratios of 0.5 and 0.35 were hydrated at 30 °C and 50 °C for up to six months. The glass fraction of slag was 0.97. After curing periods of 3, 7, 14, 28, 90 and 180 days, the percentage of reacted slag, and the amounts of chemically-bound water and calcium hydroxide were determined.

4.2.1. The percentage of reacted slag

The percentage of reacted slag was estimated using a selective dissolution method based on the extraction of the constitutes other than the unreacted slag with a reagent based on ethylene diamine tetraacetic acid (EDTA). Based on the reacted slag ratios at different curing temperatures, the reaction coefficients of Eq. (12) were determined. (As B_{SL} = 1e−9 cm/h, C_{SL} = 0.004 cm/h, D_{eSL0} = 5.846e−9 cm^2/h and k_{rSL} = 7.081e−6 cm/h, respectively, at 30 °C. The activation energies of B_{SL}, C_{SL}, k_{rSL} and D_{eSL0} were 10, 800, 6500 and 4000, respectively.) The evolution of the reacted slag ratio is shown as a function of hydration time in Fig. 6. As seen in this figure, the calibration results were in accordance with the experimental results.

Subsequently, the influences of curing temperature, water to binder ratio and slag replacement ratio on the reaction ratio of slag were considered. First, we increased the curing temperature of the cement–slag paste from 30 °C (results shown in Fig. 6a, c and e) to 50 °C (results shown in Fig. 6b, d, and f); the reactivity of slag also increased. Second, increasing the water to binder ratio from 0.35 (results shown in Fig. 6c and d) to 0.5 (results shown in Fig. 6e

Table 1
Hydration coefficients of the proposed model.

B	C	k_{rc3s}	k_{rc2s}	k_{rc3a}	k_{rc4af}	D_{ec3s0}	D_{ec3a0}	D_{ec2s0}	D_{ec4af0}
2E−9	1.5E15	2.422E−5	1.815E−7	1.985E−6	3.759E−7	6.328E−10	9.568E−8	6.328E−10	9.568E−8
β_1	$\frac{E_{c3s}}{R}$	$\frac{E_{c2s}}{R}$	$\frac{E_{c3a}}{R}$	$\frac{E_{c4af}}{R}$	β_{2c3s}	β_{2c3a}	β_{2c2s}	β_{2c4af}	
89	6000	3500	7000	3000	3500	4500	3500	4500	

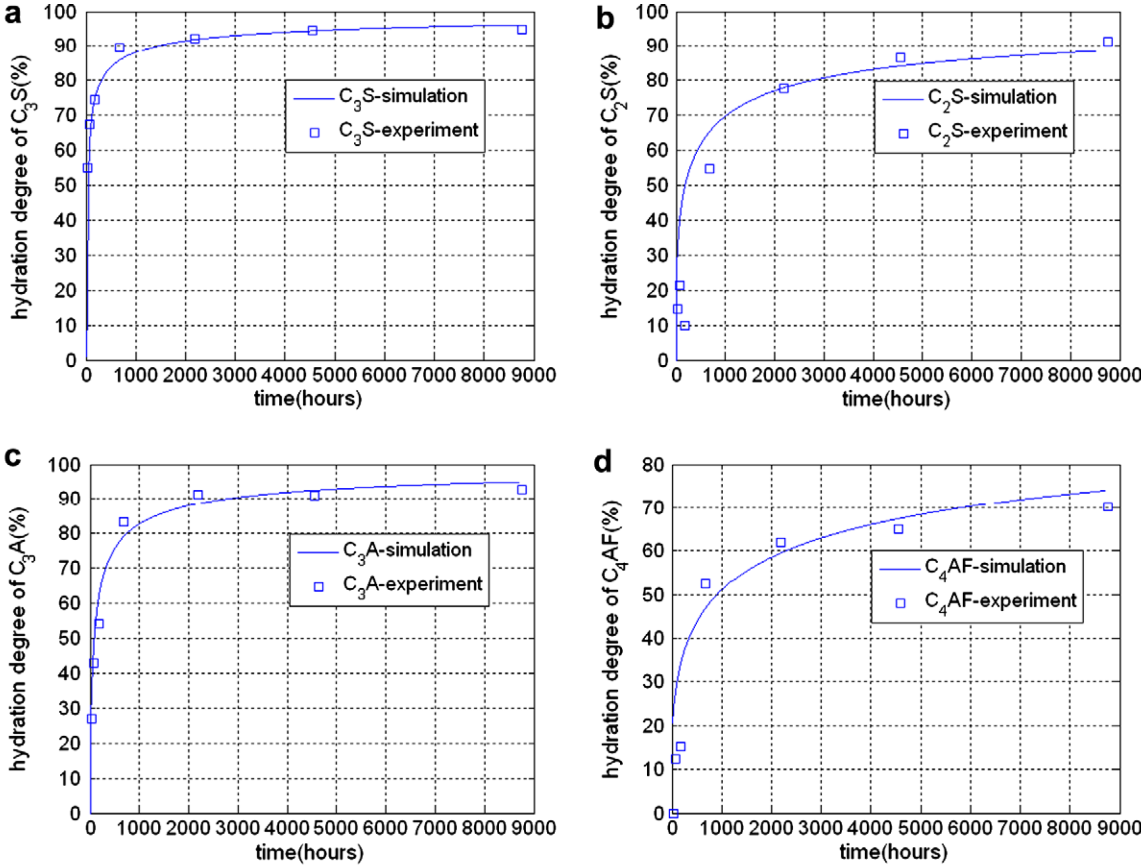

Fig. 3. Simulated and measured hydration degrees of cement mineral components: (a) C_3S; (b) C_2S; (c) C_3A; and (d) C_4AF.

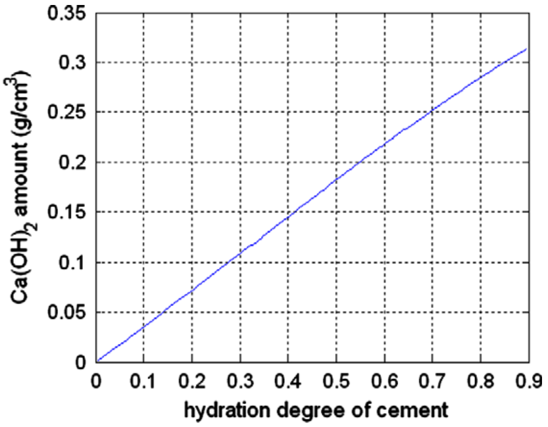

Fig. 4. Calculated CH amount as a function of degree of hydration.

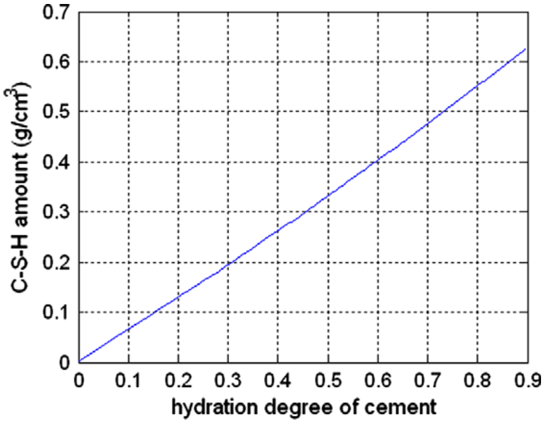

Fig. 5. Calculated C–S–H amount as a function of degree of hydration.

and f) resulted in more available space in which the hydration product could form, hence a corresponding increase in slag reactivity. Third, the slag replacement level was reduced from 50% (results shown in Fig. 6c and d) to 30% (results shown in Fig. 6a and b), resulting in a greater alkaline activating effect for the cement, which also caused an increase in slag reactivity.

Generally speaking, a model should include calibration part and validation part. In this paper, the calibration of parameters is based on the degree of reaction of mineral compositions of cement and reaction ratio of slag. The evolution of properties of slag–blended concrete can be evaluated by considering the contributions from both the hydration of cement and the reaction of slag. The evaluation of properties of slag–blended concrete is the validation part. The calibration and validation processes of the hydration model parameters were as follows.

Initially, based on the experimental results of the degree of reaction of the mineral components in Portland cement using different curing temperatures, the parameters related to the reaction rate of each of the mineral components were calibrated, and these parameters are shown in Table 1. In this process, a predictor–corrector algorithm was adopted in order to confirm the values of the coefficients [17]. This algorithm consisted of two steps: first, the prediction step calculated a rough approximation of the desired quantity; second, the corrector step refined the initial approxima-

Table 2
Mineral compositions of the Portland cement.

	Mineral composition (mass%)					Blaine (cm^2/g)
	C_3S	C_2S	C_3A	C_4AF	$C\bar{S}_2H$	
OPC	70.5	12.0	3.5	10.5	2.5	3765

Table 3
Chemical compositions of the slag.

	Chemical composition (mass%)						Blaine (cm^2/g)
	SiO_2	Al_2O_3	Fe_2O_3	CaO	MgO	SO_3	
Slag	35.3	11.4	1.7	33.9	13.8	0.0	3400

tion through other means. Using the parameters, the degrees of hydration of Portland cement with different mineral components and particle size distributions can be evaluated as a function of curing age [17,26]. Furthermore, the development of early-age mechanical behaviors can be evaluated [17,23].

Moreover, in the hydrating cement–slag blends, two reactions, the hydration of cement and the reaction of slag, coexist. The contribution of Portland cement hydration can be evaluated using the parameters obtained from the first step. Based on the experimental results pertaining to the reaction ratio of slag at different curing temperatures and the predictor–corrector algorithm, the parameters relating to the slag reaction were able to be calibrated. The fit parameters for slag depend on its physical and chemical characteristics and do not change in the various mix proportions.

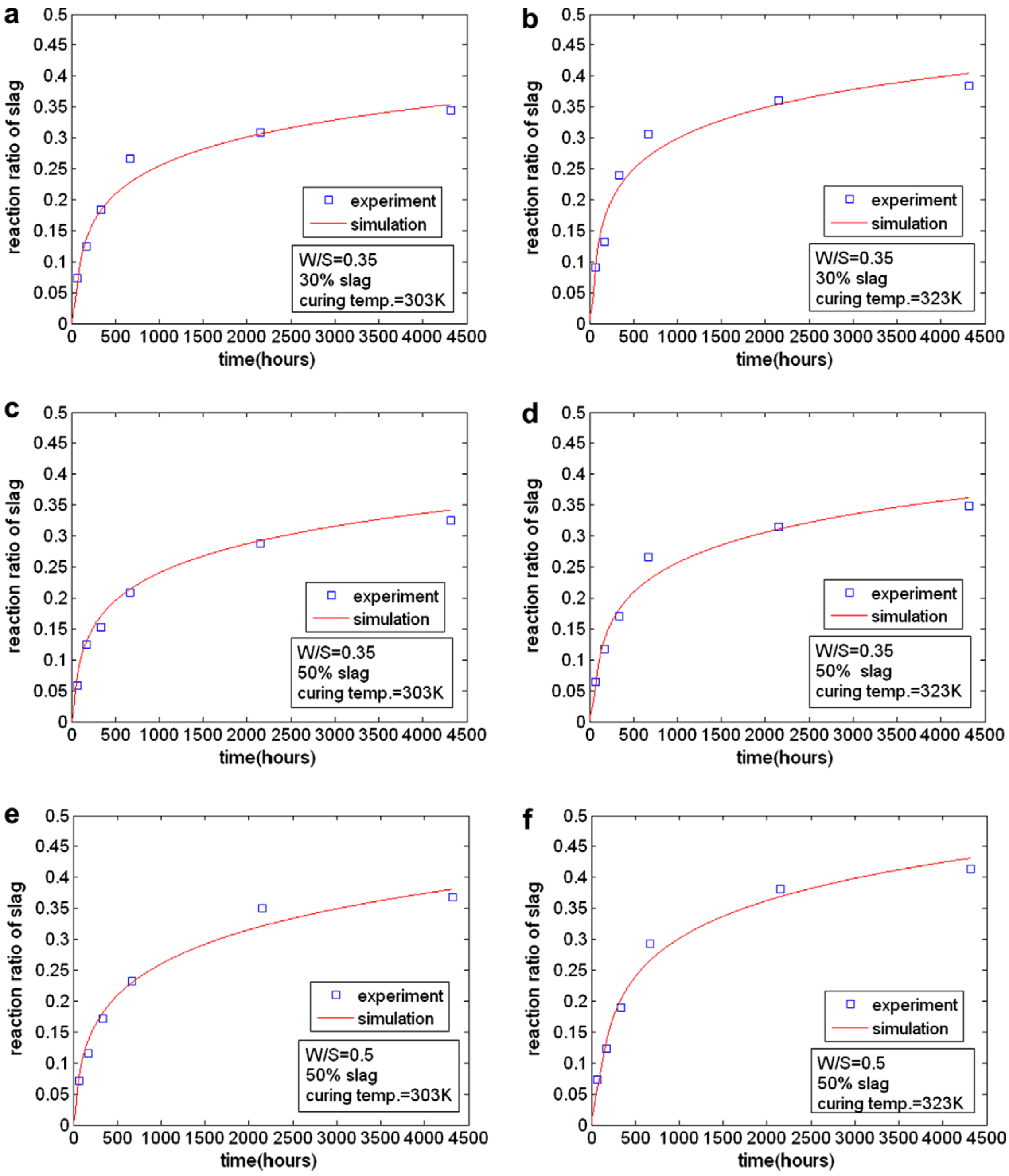

Fig. 6. Simulated and measured reaction degrees of slag.

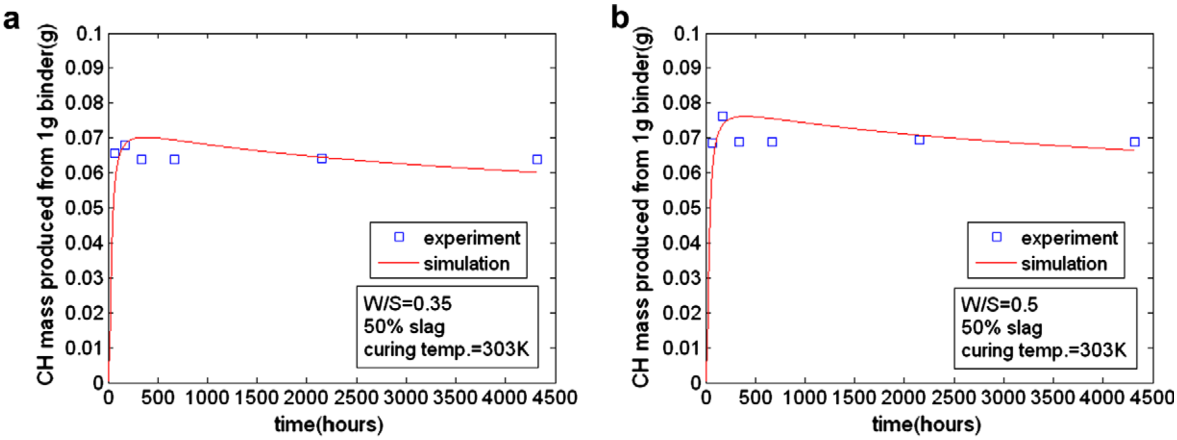

Fig. 7. Simulated and measured amounts of calcium hydroxide.

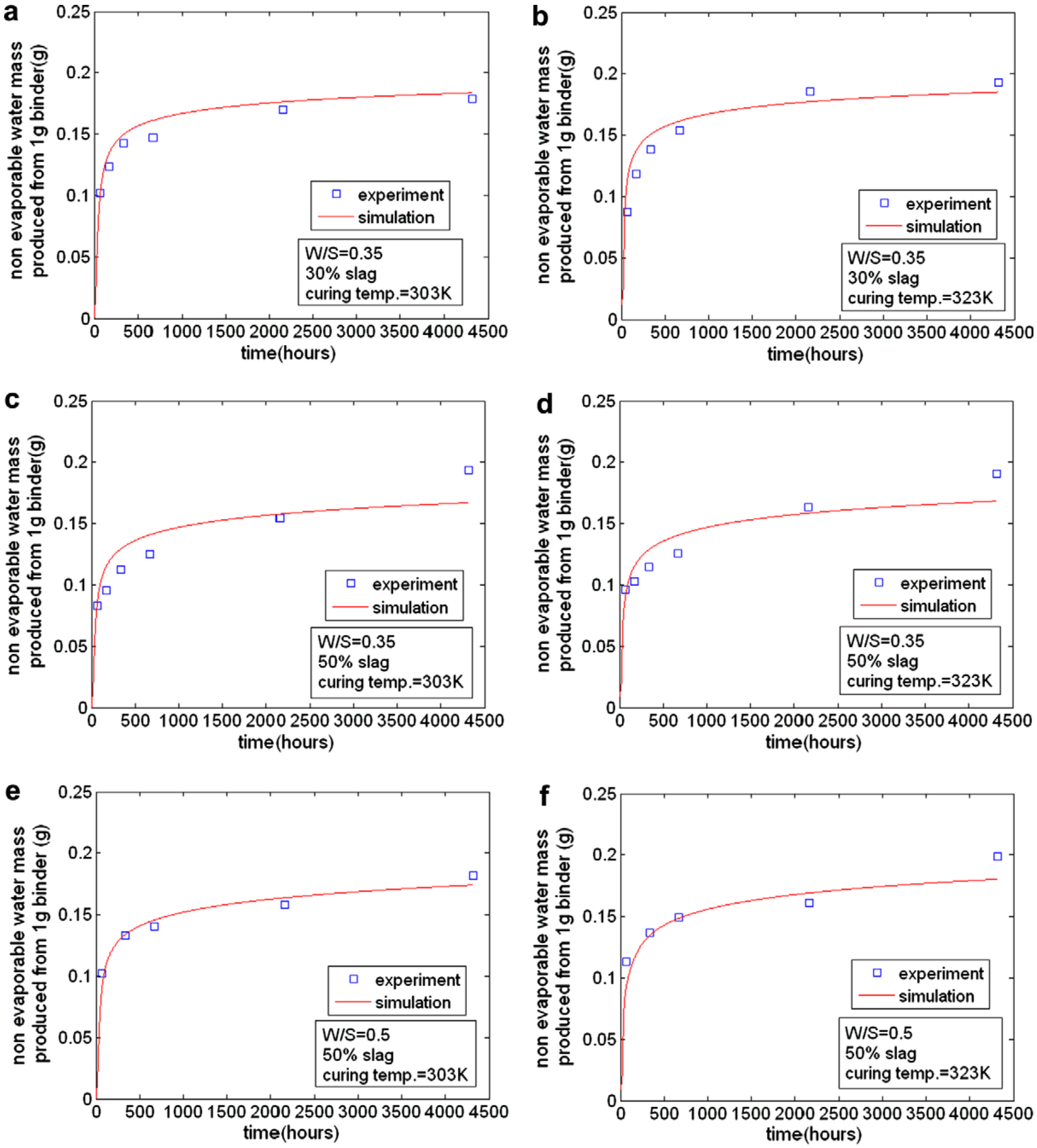

Fig. 8. Simulated and measured amounts of chemically-bound water.

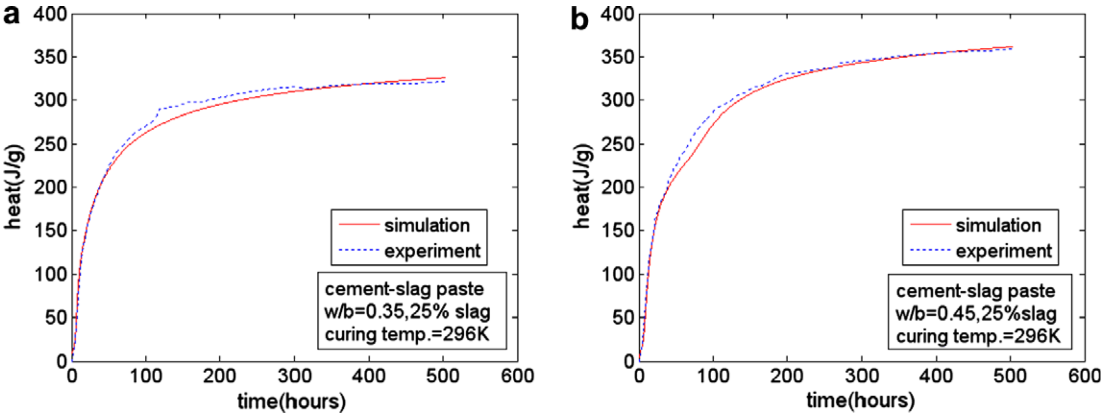

Fig. 9. Simulated and measured heat production due to cement–slag paste hydration.

Finally, based on the parameters obtained in steps 1 and 2, the properties of hydrating cement–slag blends, such as the chemically-bound water amount, the calcium hydroxide amount, and the released heat of hydration, could be evaluated in light of the contributions from both cement hydration and slag reaction [34–36].

4.2.2. Calcium hydroxide amounts during the hydration period

In the experiment, the calcium hydroxide was estimated by means of a thermal analysis using a thermo-balance. Samples of 35 mg were heated at 15 °C/min to 900 °C. The amount of calcium hydroxide was estimated from the weight loss at 450–550 °C [33]. In the hydration of ordinary Portland cement, the mass of calcium hydroxide will increase until a steady state is reached. In the hydration of cement–slag blends, the evolution of the CH mass depends on two factors, the Portland cement hydration that produces CH and the reaction of slag that consumes CH. When slag replaces cement to a high percentage, the CH content may pass through a maximum level and then decrease. The evolution of the mass of CH is shown as a function of the hydration time in Fig. 7, which also shows that the calculated results were in accordance with the experimental results.

4.2.3. Chemically-bound water amounts during the hydration period

The chemically-bound water was estimated from the ignition loss at 950 °C Samples of 1 g were weighted with a 0.0001 precision, dried at 130 °C for one hour and then heated at 950 °C for 20 min [33]. Chemically-bound water provides a quantitative indicator of the cement's hydration. For blended cements, both the cement and slag reactions contribute to the value. By considering the production of CH in cement hydration and the consumption of CH in the slag reaction, the proposed hydration model was able to separate the slag reaction from cement hydration. Furthermore, the contributions of slag and cement to chemically-bound water can be determined. The evolution of the mass of chemically-bound water is shown as a function of hydration time in Fig. 8, which also shows that the calculated results correspond well with the experimental results. The differences between the calculated results and the experimental results could be attributed to the estimation of the stoichiometry of the slag reaction and the difference in the mineral component reaction rates of the slag [7–10].

4.2.4. The heat released during the hydration period

The proposed model was employed to determine the amount of heat released for cement–slag blends [34]. The released heat was measured by isothermal calorimetry. The water to binder ratios (*w*/*b*) was 0.35 and 0.45, respectively, the slag substation rate was 25%, and the curing temperature of the slag–cement paste was 23 °C. In our simulation the released heat of the hydrating cement–slag blends was obtained from the sum of the individual components. Based on the proposed hydration model, the heat evolution was shown as a function of hydration time (Fig. 9). As illustrated in Fig. 9, the prediction results are in general agreement with the experimental results. The differences between the experimental and simulation results could possibly be attributed to the facts that slag's retardation and nucleation effects on cement hydration were not considered in the proposed model, and in the simulation the particle size distribution of slag was simplified to "monosize." Smaller-sized slag particles have a much higher reactivity than do medium-sized ones [35].

5. Conclusions

In this paper, two kinetic equations are employed to describe the reactions of cement and slag, respectively. By considering the production of calcium hydroxide in cement hydration and its consumption in the slag reaction, the proposed model was able to separate the two reactions. Similar to the hydration reaction of cement, slag activity was divided into three processes: as an initial dormant period, a phase-boundary reaction process and a diffusion process. The mutual interactions between the cement hydration and slag reaction are considered through the available calcium hydroxide amount and available capillary water amount in system. The amounts of capillary water and calcium hydroxide left in the system were adopted as the control indicators for determining slag reaction. The fit parameters do not change from one mix to another, and depend only on physical and chemical characteristic of slag. Both the early-age properties and long-term durability can be evaluated with proposed model.

By applying the proposed model, the reaction ratio of slag was evaluated as a function of the curing age, considering the influences of the water to binder ratio, the slag replacement ratio and the curing temperature. Through the modeling efforts, some insights were gained into the reaction of cement–slag blends: the reactivity of slag increases at higher temperatures; with an increase of water to binder ratio, there is more space available for hydration products to form, hence the reactivity of slag increases correspondingly; with a reduction of the replacement level of slag, the alkaline activating effect of the cement would be greater, so that the reactivity of slag will increase.

Furthermore, based on the reaction ratio of cement and slag, the amounts of chemically-bound water (self-cementing properties), calcium hydroxide (pozzolanic capabilities), and the released heat of hydration were evaluated by considering the contributions of both cement hydration and the slag reaction.

Acknowledgements

The authors are grateful to reviewers for their valuable suggestions and comments. This study was supported by the Engineering Research Center designated by the Ministry of Education and Science Technology, Sustainable Building Research Center, Hanyang University (R11-2005-056-04003). This research was supported by a Grant (06-CIT-A02: Standardization Research for Construction Materials) from Construction Infrastructure Technology Program funded by Ministry of Land, Transport and Marine Affairs.

References

[1] Metha PK, Monteiro PJM. Concrete: microstructure, properties and materials. 3rd ed. New York: McGraw-Hill; 2006.

[2] Taylor HFW. Cement chemistry. 2nd ed. London: Thomas Telford; 1997.

[3] Shi CJ, Day RL. A calorimetric study of early hydration of alkali–slag cement. Cem Concr Res 1995;25(6):1333–46.

[4] Song S, Sohn D, Jennings HM, Mason TO. Hydration of alkali-activated ground granulated blast furnace slag. J Mater Sci 2000;35(1):249–57.

[5] Wang SD, Scrivener KL. Hydration products of alkali activated slag cement. Cem Concr Res 1995;25(3):561–71.

[6] Chen W, Brouwers JH. The hydration of slag, part 1: reaction models for alkali–activated slag. J Mater Sci 2007;42(2):428–43.

[7] Papadakis VG. Effect of supplementary cementing materials on concrete resistance against carbonation and chloride. Cem Concr Res 2000;30(2):291–9.

[8] Papadakis VG, Tsimas S. Supplementary cementing materials in concrete, part I: efficiency and design. Cem Concr Res 2002;32(10):1525–32.

[9] Papadakis VG, Fardis MN, Vayenas CG. Hydration and carbonation of pozzolanic cements. ACI Mater J 1992;89(2):119–30.

[10] Papadakis VG, Antiohos S, Tsimas S. Supplementary cementing materials in concrete, part II: a fundamental estimation of the efficiency factor. Cem Concr Res 2002;32(10):1533–8.

[11] Schindler AK, Folliard KJ. Heat of hydration models for cementitious materials. ACI Mater J 2005;102(1):24–33.

[12] De Schutter G, Taerwe L. General hydration model for Portland cement and blast furnace slag cement. Cem Concr Res 1995;25(3):593–604.

[13] De Schutter G, Taerwe L. Degree of hydration-based description of mechanical properties of early age concrete. Mater Struct 1996;29(6):335–44.

[14] De Schutter G. Hydration and temperature development of concrete made with blast-furnace slag cement. Cem Concr Res 1999;29(1):143–9.

[15] De Schutter G. Fundamental study of early age concrete behavior as a basis for durable concrete structures. Mater Struct 2002;35(1):15–21.

[16] De Schutter G. Finite element simulation of thermal cracking in massive hardening concrete elements using degree of hydration based material laws. Comput Struct 2002;80(27–30):2035–42.

[17] Hyun C. Prediction of thermal stress of high strength concrete and massive concrete. PhD thesis. Tokyo: The University of Tokyo; 1995.

[18] Tomosawa F, Noguchi T, Hyun C. Simulation model for temperature rise and evolution of thermal stress in concrete based on kinetic hydration model of cement. In: Glasser FS, Justnes H, editors. Proceedings of 10th international congress chemistry of cement (ICCC), vol. 4. Gothenburg, Sweden; 1997. p. 72–5.

[19] Maekawa K, Chaube R, Kishi T. Modeling of concrete performance: hydration, microstructure formation and mass transport. London and New York: Routledge; 1998.

[20] Di Luzio G, Cusatis G. Hydro–thermo-chemical modeling of high performance concrete, I: theory. Cem Concr Compos 2009;31(5):301–8.

[21] Di Luzio G, Cusatis G. Hydro–thermo-chemical modeling of high performance concrete, II: numerical implementation, calibration and validation. Cem Concr Compos 2009;31(5):309–24.

[22] Navi P, Pignat C. Simulation of cement hydration and the connectivity of the capillary pore space. Adv Cem Mater 1996;4(1):58–67.

[23] Park KB, Noguchi T, Plawsky J. Modeling of hydration reaction using neural network to predict the average properties of cement paste. Cem Concr Res 2005;35(9):1676–84.

[24] Tomosawa F. Development of a kinetic model for hydration of cement. In: Glasser F S, Justnes H, editors. Proceedings of the 10th ICCC, vol. 2. Gothenburg; 1997. p. 51–8.

[25] Brouwers HJH. The work of Powers and Brownyard revisited: part 1. Cem Concr Res 2004;34(10):1697–716.

[26] Maruyama I. Numerical model for hydration of Portland cement. In: Proceedings of the international conference of civil and environmental engineering, Hiroshima; 2003. p. 53–62.

[27] Gutteridge WA, Dalziei JA. Filler cement: the effect of the secondary component on the hydration of Portland cement. Cem Concr Res 1990;20(5):853–61.

[28] Paine KA, Zheng L, Dhir PK. Experimental study and modeling of heat evolution of blended cement. Adv Cem Res 2005;17(3):121–32.

[29] Takemoto K, Uchikawa H. Hydration of pozzolanic cement. In: Proceedings of 7th international congress on the chemistry of cement, vol. 1. Paris; 1980. p. iv-2/1–/29 [principal reports].

[30] Escalante JI, Sharp JH. The microstructure and mechanical properties of blended cements hydrating at various temperatures. Cem Concr Res 2001;31(5):695–702.

[31] Saeki T, Monteiro PJM. A model to predict the amount of calcium hydroxide in concrete containing mineral admixture. Cem Concr Res 2005;35(10):1914–21.

[32] Matsushita T, Hoshino S, Maruyama I, Noguchi T, Yamada K. Effect of curing temperature and water to cement ratio on hydration of cement compounds. In: Beaudoin J, editor. Proceedings of 12th international congress on the chemistry of cement, Montreal; 2007 [TH2-07.3].

[33] Escalante JI, Gomez LY, Johal KK, Mendoza G, Mancha H, Mendez J. Reactivity of blast furnace slag in Portland cement blends hydrated under different conditions. Cem Concr Res 2001;31(10):1403–9.

[34] Pane I, Hansen W. Investigation of blended cement hydration by isothermal calorimetry and thermal analysis. Cem Concr Res 2005;35(6):1155–64.

[35] Wang XY, Lee HS, Park KB. Simulation of low-calcium fly ash blended cement hydration. ACI Mater J 2009;106(2):;167–175.

[36] Lam L, Wong YL, Poon CS. Degree of hydration and gel/space ratio of high-volume fly ash/cement systems. Cem Concr Res 2000;30:747–56.